Energy Nexus 20 (2025) 100583

Contents lists available at ScienceDirect

Energy Nexus

journal homepage: www.elsevier.com/locate/nexus

A synergistic framework integrating statistical design and machine learning for enhancing biogas yield

Yuxuan Li [a], Mahuizi Lu [b], Luiza C. Campos [a], Shikun Cheng [c], Zifu Li [c], Yukun Hu [a,*]

[a] Department of Civil, Environmental & Geomatic Engineering, University College London, London WC1E 6BT, United Kingdom
[b] Department of Earth Science and Engineering, Imperial College London, London SW7 2BX, United Kingdom
[c] School of Energy and Environmental Engineering, Beijing Key Laboratory of Resource-Oriented Treatment of Industrial Pollutants, University of Science and Technology Beijing, Beijing 100083, China

ARTICLE INFO

Keywords:
Machine learning algorithms
Response surface methodology
Microwave pretreatment
Nonthermal Effects
Biogas yield

ABSTRACT

Anaerobic digestion (AD) of waste-activated sludge is hindered by slow hydrolysis and complex sludge structure, which limit biogas recovery and threaten process stability. Although pretreatment methods such as microwave pretreatment (MP) have shown promise, their energy efficiency and underlying nonthermal effects remain poorly understood. In parallel, existing predictive models often neglect pretreatment conditions, restricting their applicability for process optimization. To bridge these gaps, this study proposes a synergistic framework that integrates statistical optimization with advanced machine learning (ML) to enhance biogas production from MP-assisted AD. Response Surface Methodology (RSM) identified optimal pretreatment conditions—holding time, pH, total solids (TS%), and microwave power—predicting a cumulative biogas yield (CBY) of 1020.5 mL/gVS, closely validated by experiments (1013.8 mL/gVS). These optimized datasets were further used to train ensemble ML models (AdaBoost, LightGBM, XGBoost), achieving high predictive accuracy (XGBoost $R^2 = 0.992$) with strong external validation. SHapley Additive exPlanations (SHAP) revealed TS% as the dominant factor, contrasting with RSM's linear emphasis on microwave power, thereby highlighting nonlinear interactions and hidden effects. Complementary fluorescence microscopy and ImageJ analysis confirmed microwave-induced structural disruption of extracellular polymeric substances (EPS) and microbial accessibility, particularly at moderate power (600 W), evidencing distinct nonthermal contributions. By combining RSM's statistical optimization with ML's predictive and interpretive capacity, this framework not only refines operational conditions for maximum yield but also elucidates the mechanisms of MP, balancing energy input and performance. These insights support the design of more energy-efficient, scalable, and sustainable AD systems.

1. Introduction

Anaerobic digestion (AD) has emerged as a promising method for managing waste-activated sludge (WAS), providing a sustainable means to generate renewable energy in the form of biogas while reducing environmental impacts associated with traditional sludge disposal methods such as landfilling and incineration [1,2]. However, AD efficiency remains limited by slow hydrolysis rates and the complex structural integrity of sludge components [3], primarily due to extracellular polymeric substances (EPS), necessitating effective pretreatment technologies to enhance microbial access to substrates [4,5]. Microwave pretreatment (MP) has been recognized as an effective technique, offering rapid and uniform heating alongside unique non-thermal interactions that can significantly enhance sludge digestibility compared to conventional heating methods [6,7]. However, despite MP holding promising potential, the economic sustainability of AD facilities poses a considerable challenge, often exacerbated by process instabilities leading to operational failures. In this context, process modelling has become an indispensable tool for predicting key performance indicators, such as methane yield [8], thereby improving the predictability and reliability of AD operations [9].

Machine learning (ML), particularly advanced ensemble algorithms such as AdaBoost, LightGBM, and XGBoost, has shown strong capabilities in capturing complex nonlinear interactions within anaerobic digestion processes [10,11]. However, most existing studies applying these ML techniques to anaerobic digestion have focused mainly on predicting biogas yields from operational parameters alone, largely

* Corresponding author.
E-mail address: yukun.hu@ucl.ac.uk (Y. Hu).

https://doi.org/10.1016/j.nexus.2025.100583
Received 25 March 2025; Received in revised form 8 October 2025; Accepted 17 November 2025
Available online 19 November 2025

Nomenclature and Abbreviations

A	Holding time (min)
AD	Anaerobic Digestion
AMPTS II	Automatic Methane Potential Test System
ANN	Artificial Neural Network
ANOVA	Analysis of Variance
B	pH value
BBD	Box–Behnken Design
CBY	Cumulative Biogas Yield
CH	Conventional Heating
C	Total Solids (%)
CCD	Central Composite Design
COD	Chemical Oxygen Demand
D	Microwave power (W)
DAPI	4′,6-diamidino-2-phenylindole
DoE	Design of Experiments
EPS	Extracellular Polymeric Substances
FITC	Fluorescein Isothiocyanate
FTIR	Fourier Transform Infrared Spectroscopy
gVS	grams of Volatile Solids
LGBM	Light Gradient Boosting Machine
GFP	Green Fluorescent Protein filter set
MAE	Mean Absolute Error
ML	Machine Learning
MP	Microwave Pretreatment
MW	Microwave
MW 600/MW 1000	Microwave at 600 W / 1000W
Original	No Pretreatment
PH1	Phase Contrast mode
p-value	Probability Value
R^2	Coefficient of Determination
RMSE	Root Mean Square Error
2D	Two-dimensional
ROI	Region of Interest
RSM	Response Surface Methodology
SCOD	Soluble Chemical Oxygen Demand
SHAP	SHapley Additive exPlanations
TCOD	Total Chemical Oxygen Demand
TS	Total Solids
VS	Volatile Solids
WAS	Waste Activated Sludge
XGB	Extreme Gradient Boosting
3D	Three-dimensional

overlooking pretreatment processes and their detailed impacts on sludge digestibility and microbial interactions [12,13]. This limited scope restricts their practical utility in optimizing pretreatment-based enhancements to biogas production.

To bridge these methodological gaps, the current study integrates statistical optimization using Response Surface Methodology (RSM) with advanced ML predictive analysis to optimize MP conditions for enhancing biogas yield. This combined framework utilizes the strength of RSM in systematically identifying optimal parameter ranges [14], while ML algorithms validated through rigorous cross-validation capture complex nonlinear interactions among variables, including nonthermal effects often neglected by conventional approaches. By critically synthesizing previous research and overcoming limitations such as narrow application scopes and insufficient validation, this study establishes a robust and scalable methodological framework that improves predictive accuracy and operational efficiency in microwave-assisted AD systems.

Accordingly, this study aims to enhance biogas production from waste-activated sludge by integrating experimental, statistical, and data-driven modelling approaches. The specific objectives are: (1) to experimentally evaluate thermal and nonthermal microwave pretreatment effects at different power levels; (2) to develop ML models (AdaBoost, LGBM, XGBoost) for accurate prediction of cumulative biogas yield; (3) to identify key operational variables using SHAP-based feature importance analysis; and (4) to optimize process parameters using RSM. This study ultimately aims to provide actionable insights and scalable solutions for sustainable energy recovery from sludge treatment.

2. Material and methods

2.1. Chemical analysis

The following parameters were analysed in the solid fraction of WAS: TS and volatile solids (VS) were measured according to standard methods [15]. The samples were centrifuged at 8000 rpm for 10 min and subsequently filtered through a 0.45μm cellulose membrane [16]. The pH of the filtrate was then measured using a pH meter (pHs-3C, Leici Co. Ltd., Shanghai). Soluble chemical oxygen demand (SCOD) and total chemical oxygen demand (TCOD) were quantified using a visible light spectrophotometer (DR3900, HACH, USA). All chemical analyses were performed in triplicate to ensure reliability, and results are presented as mean ± standard deviation.

2.2. Fluorescence and brightfield microscopy

Fluorescence and brightfield microscopy were performed using a Nikon Ti2 inverted fluorescence and brightfield microscope (Nikon Instruments, Japan) to analyse sludge microstructure and microbial aggregation under different pretreatment conditions. The imaging was conducted at 10 × magnification using 4′,6-diamidino-2-phenylindole (DAPI) triple (blue) and green fluorescent protein (GFP) triple (green) filter sets, together with brightfield phase contrast (PH1) mode for enhanced structural visualization. The microscope was configured with a 16-bit dynamic range, a region of interest (ROI) of 2720 pixels, and an auto-exposure time of 200 ms.

Two fluorescent dyes were used to selectively stain sludge components:

- Calcofluor White (Merck Life Science Limited, Germany) was applied to stain EPS and polysaccharides in the sludge matrix. This fluorochrome binds specifically to β-linked polysaccharides and emits blue fluorescence when excited. Samples were incubated with Calcofluor White for 30 minutes, and fluorescence was captured using the DAPI filter set.
- Fluorescein Isothiocyanate (FITC, Bio-Techne, USA) was used to stain proteins and microbial cell structures, allowing differentiation between microbial cells and the surrounding sludge matrix. FITC emits green fluorescence upon excitation. Sludge samples were stained with FITC for 60 min, and fluorescence was recorded using the GFP filter set.

All imaging parameters, including exposure settings and fluorescence intensities, were kept consistent across all samples to ensure comparability. Brightfield microscopy in PH1 mode was also applied to provide additional structural context.

2.3. Experimental samples and properties

The raw WAS, used as the substrate, was collected from a municipal wastewater treatment plant in Jinchang, China, which operates using anaerobic/anoxic/oxic processes (Figure S1). The sludge was sampled after sedimentation and centrifugation. The inoculum was sourced from a laboratory-scale mesophilic AD reactor. The primary analytical characteristics of both the substrate and inoculum are presented in Table 1. Sludge samples were transported to the laboratory in a polypropylene plastic container, passed through a 1.0 mm sieve, and stored at 4 °C in a refrigerator until further use.

2.4. Experimental setup and procedures

2.4.1. Microwave pretreatment

The microwave irradiation was applied to the WAS substrate using a household microwave oven (John Lewis, JLSMWO09, UK) operating at a frequency of 2450 MHz. Based on preliminary studies and established literature [6,17], four critical parameters were identified as significant in influencing microwave pretreatment efficacy: holding time, pH, total solids (TS %), and microwave power. These parameters were systematically tested within the following ranges to determine their optimal conditions: microwave power (600, 800, and 1000 W), holding time (3, 6, and 9 min), pH (5, 7, and 9), and TS % (4 %, 6 %, and 8 %), as justified by prior studies that demonstrated these ranges effectively influence biogas yield through enhanced substrate accessibility and microbial activity [18].

For each pretreatment run, sludge samples were placed in microwave-safe glass vessels and subjected to microwave irradiation at the predetermined power level and holding time. Immediately after irradiation, samples were allowed to cool to room temperature naturally (approximately 22 ± 2 °C), without external cooling, to avoid additional variability in microbial structure due to rapid cooling. Following cooling, samples were gently mixed with inoculum sludge at a substrate-to-inoculum ratio of 3:1 before transferring into anaerobic digesters for further experimentation [19], as described in the subsequent sections. The experimental setup is shown in Figure S2.

AD was conducted using the Automatic Methane Potential Test System (AMPTS II; Bioprocess Control, Sweden), which provided real-time measurements of biogas production over a period of 20–40 days [20]. The digester was mixed using a motor-driven stirring rod, operating at a rotation speed of 80 rpm with an agitation frequency of 60 s ON and 60 s OFF. The produced biogas was directed through flexible tubing to a scrubbing reactor, where acid gases (CO_2, H_2S) were removed using a 4 M NaOH alkali solution. The remaining methane was then passed into a measuring cell equipped with a gas counter based on liquid displacement, which recorded gas impulses and converted them into normalised millilitres of CH_4 per gram of volatile solids (mL/gVS) using AMPTS® v5 software [21]. The experiments were conducted under mesophilic conditions at 37.5 °C to evaluate the impact of MP on biogas production, with continuous tracking of biogas yield.

2.4.2. Experimental design

This study adopts a dual-phase analytical approach to enhance the prediction and optimization of biogas yield in microwave-assisted AD processes. First, RSM is employed to optimize response variables within the multi-dimensional parameter space of the MP process, aiming to identify the optimal operational conditions for improved methane yield. In the second phase, advanced ML models, including AdaBoost, LGBM, and XGB, are utilised to predict biogas yields, capitalising on their ability to manage complex nonlinear relationships. The predictive accuracy of these models is compared to validate the optimization findings and to advance predictive analytics in this context.

Table 1
Key physicochemical characteristics of the experimental samples.

Parameters	Sludge	Inoculum
Moisture content (%)	92.21±0.46	93.06±0.03
Total Solid (g/L)	77.90±4.60	69.36±0.08
Volatile Solid (g/L)	46.64±11.67	55.21±0.06
Total Chemical Oxygen Demand (g/L)	17.41±1.54	28.46±0.49
Soluble Chemical Oxygen Demand (g/L)	3.93±0.49	5.22±0.18
pH	6.64 ± 0.12	6.92 ± 0.13

2.4.3. Box-Behnken design coupled with RSM

In this context, the Design of Experiments (DoE) methodology [22] provides a crucial framework, enabling precise and efficient navigation through complex experimental setups. The application of DoE principles during the developmental stages of a process not only reduces operational costs but also conserves valuable time, thus enhancing the research trajectory towards its objectives [23]. In this study, four key parameters, i.e. TS % content (A), microwave power (B), microwave holding time (C), and pH (D), were selected based on prior research for their influence on methane production and MP [24–26]. The TS % was adjusted by dilution with deionized water or concentration via centrifugation, while pH was controlled using 4 mol/L HCl and NaOH standard solutions.

Central to this experimental design is RSM, a robust statistical toolset used to model and analyse the effects of multiple independent variables on a response variable [27]. RSM is effective in identifying optimal conditions as it minimises experimental costs and computational errors, and efficiently addresses confounding variables [28]. In this study, the Box–Behnken Design (BBD) was selected over the traditional Central Composite Design (CCD) due to its efficiency and suitability for biological processes such as anaerobic digestion [29]. Unlike CCD, which includes extreme experimental conditions that may lead to process instability, BBD focuses on mid-range values, reducing the likelihood of operational failures [30]. Additionally, BBD requires fewer experimental runs while effectively capturing quadratic and interaction effects among variables, making it both cost-effective and statistically robust for optimizing biogas production parameters [31]. The experimental design involves four factors, each at three levels, allowing for a comprehensive exploration of the experimental domain with 29 runs. This approach enables a balanced assessment of main effects, interactions, and quadratic effects without the need for extreme conditions that could compromise process performance or results, as detailed in Table S1. The model equation for the RSM–BBD is presented in Eq. (1).

$$Y = \beta_0 + \sum_{i=1}^{n} \beta_i x_i + \sum_{i=1}^{n} \beta_{ii} x_i^2 + \sum_{i=1}^{n} \sum_{j>i}^{n} \beta_{ij} x_i x_j \tag{1}$$

Where Y is the predicted response variable, representing the outcome of the model (cumulative biogas yield); β_0 is the model constant; x_i,x_j are the independent variables representing the coded levels of factors; β_i are the linear coefficients; β_{ii} are the quadratic coefficients for the squared terms; and β_{ij} are the interaction coefficients representing the interactions between the independent variables. The summation over i and j accounts for all variable interactions, with $j > i$ to avoid redundant combinations [32].

By applying the least-squares method to solve this equation, the correlation coefficients can be computed, enabling the development of a practical quadratic polynomial model. This model effectively interprets the experimental data derived from the 29 runs, providing a detailed analysis of the effects and interactions between the variables under study. Through this methodological approach, our investigation identifies the optimal conditions that maximize the response variable, demonstrating the efficacy of the Box-Behnken design in facilitating a systematic exploration of the experimental space with an optimized number of runs.

2.4.4. Machine learning approaches

In the present study, the objective is to predict biogas yield from AD following different MP conditions. The prediction is based on various input parameters, including mixing ratio, power level, holding time, and temperature. To achieve this, three distinct gradient boosting ML techniques are employed: AdaBoost, LGBM, and XGB. These algorithms are used for both classification and regression tasks.

AdaBoost is well-known for its simplicity and effectiveness in improving the accuracy of any given learning algorithm [33]. It achieves this by focusing on instances that are difficult-to-classify, making it highly adaptable to complex datasets. LGBM stands out for its efficiency and speed, particularly when applied to large datasets [34]. It employs gradient-based learning and is optimized for faster and more efficient performance, making it ideal for scenarios where computational efficiency is critical. XGB is celebrated for its high performance and flexibility [35]. It provides a highly scalable, portable, and efficient implementation of gradient boosting, and is a popular choice in ML competitions for delivering superior results across a range of problems.

These three algorithms were selected for their complementary strengths: AdaBoost's adaptability, LGBM's efficiency with large datasets, and XGB's exceptional performance and versatility. Together, they provide a robust framework for predicting biogas yield under various conditions, effectively leveraging the power of gradient boosting to address both classification and regression tasks.

2.4.5. Model evaluation

To rigorously evaluate the model performance and ensure robustness against overfitting, both external validation and cross-validation methods were employed. For external validation, the full dataset containing 1100 data points was randomly partitioned into a training subset (80 %, 880 data points) and a testing subset (20 %, 220 data points). The training subset was exclusively used for model development, while the testing subset, which remained entirely unseen during training, served as an independent validation set. Additionally, 5-fold cross-validation was conducted to further assess generalizability and stability of the models. In this method, the training subset was randomly divided into five equal partitions, with each partition sequentially serving once as a validation set while the remaining four partitions were used for model training. The performance metrics (Coefficient of Determination (R^2) score [36], Root Mean Square Error (RMSE) [37], and Mean Absolute Error (MAE) [38] obtained from each fold were averaged, providing an unbiased estimate of model accuracy. The evaluation metrics are mathematically expressed in Eqs. (2–4).

$$R^2 = 1 - \frac{\sum_{i=1}^{n} (y_i - \widehat{y}_i)^2}{\sum_{i=1}^{n} (y_i - \overline{y}_i)^2} \tag{2}$$

$$RMSE = \sqrt{\frac{1}{n}\sum_{i=1}^{n} (y_i - \widehat{y}_i)^2} \tag{3}$$

$$MAE = \frac{1}{n}\sum_{i=1}^{n} |y_i - \widehat{y}_i| \tag{4}$$

Where: y_i is the actual value, $\widehat{y}_i$ is the predicted value, and $\overline{y}_i$ is the mean of the actual values.

These equations form the mathematical basis for evaluating the performance of ML models in predicting biogas yield.

2.5. Analysis of the impact of input features on the target

After finalizing the ML model, the analysis was further refined by applying SHapley Additive exPlanations (SHAP), a technique inspired by cooperative game theory to provide clear interpretations of model predictions. This method uses Shapley values, derived from game theory, to break down the contribution of each input feature in influencing the model's output, assigning precise values to each feature's impact [39].

A key strength of the SHAP methodology is its highlighting of important variables and their influence by analysing the average absolute values in SHAP visualizations. Higher average SHAP values indicate that certain features have a significant effect on the model's predictions, emphasizing their crucial role. SHAP treats each data instance as a "scenario", with features acting as "participants", and the outcome as the deviation of the predicted value from the mean prediction [40]. The distribution of these outcomes, as determined by Shapley values, defines the relative influence of each feature on the prediction. Features with positive (or negative) Shapley values are interpreted as having a positive (or negative) impact on the predicted result, offering a detailed view of how different features affect the model's predictions [41].

3. Results and discussion

A total of 29 experimental runs with varied process parameters, including holding time, pH, total solids, and microwave power, are shown in Table S2. It can be inferred that variations in these parameters significantly influence the cumulative biogas yield. For instance, in runs 5 and 16, where the holding time, pH, and total solids are the same (6 min, pH 7, 8 %), but the microwave power differs (600 W and 1000 W), the biogas yields were 990.1 mL/gVS and 689.4 mL/gVS, respectively. This highlights the significant role of microwave power in optimizing biogas production. Similarly, in runs 10 and 18, where the holding time, pH, and microwave power are the same (3 min, pH 7, 800 W), but the total solids differ (8 % and 4 %), the biogas yields were 754.1 mL/gVS and 347.7 mL/gVS, respectively, emphasizing the importance of total solids in enhancing biogas yields. These results demonstrate that both total solids and microwave power are crucial factors in optimizing biogas production, aligning with findings from similar studies [17,18].

3.1. The ML-based prediction model

3.1.1. Performance evaluation

Fig. 1 presents a detailed comparative and correlative analysis of ML algorithms used to predict cumulative biogas yield (CBY) after AD. Panels (a), (c), and (e) compare actual biogas production volumes with predictions generated by AdaBoost, LGBM, and XGB, respectively, using a dataset of 1100 data points. These scatter plots visually depict the discrepancies between observed and predicted yields, illustrating the predictive strengths and limitations of each model.

In panels (b), (d), and (f), marginal histograms accompany the correlation scatter plots, providing deeper insights into the distribution of both observed and predicted values. These histograms reveal data density and variability, and further examine the alignment between predicted and actual values through regression analysis. Both XGB and LGBM exhibit high congruence with the observed data, reflecting their robust predictive capabilities, as indicated by near-unity R^2 values. In contrast, AdaBoost shows a slightly lower congruence, suggesting that while useful, it may have limitations in fully capturing the complexities of biogas yield dynamics.

The regression analysis in Fig. 1 illustrates the predictive accuracy of each model, as indicated by the slopes of the regression lines, which show how closely the predictions match actual biogas yields. Near-unity slopes for XGB and LGBM suggest these models accurately represent biogas production dynamics. However, AdaBoost's deviation from unity indicates room for model improvement, potentially through better feature selection or algorithm tuning. Additionally, the y-intercepts reveal systematic biases in the predictions. Lower intercept values, such as those for XGB, indicate minimal bias, enhancing the model's practical utility. Conversely, higher intercepts in other models may signal a need for recalibration to reduce prediction errors. This focused analysis not only highlights the effectiveness of the algorithms but also identifies key areas for improvement in model training and data handling within renewable energy research.

Table S3 summarises the performance evaluation of the three predictive models: AdaBoost, LGBM, and XGB. The R^2 values for these models are 0.816, 0.948, and 0.992, respectively, highlighting the substantial proportion of variance each model captures. These results

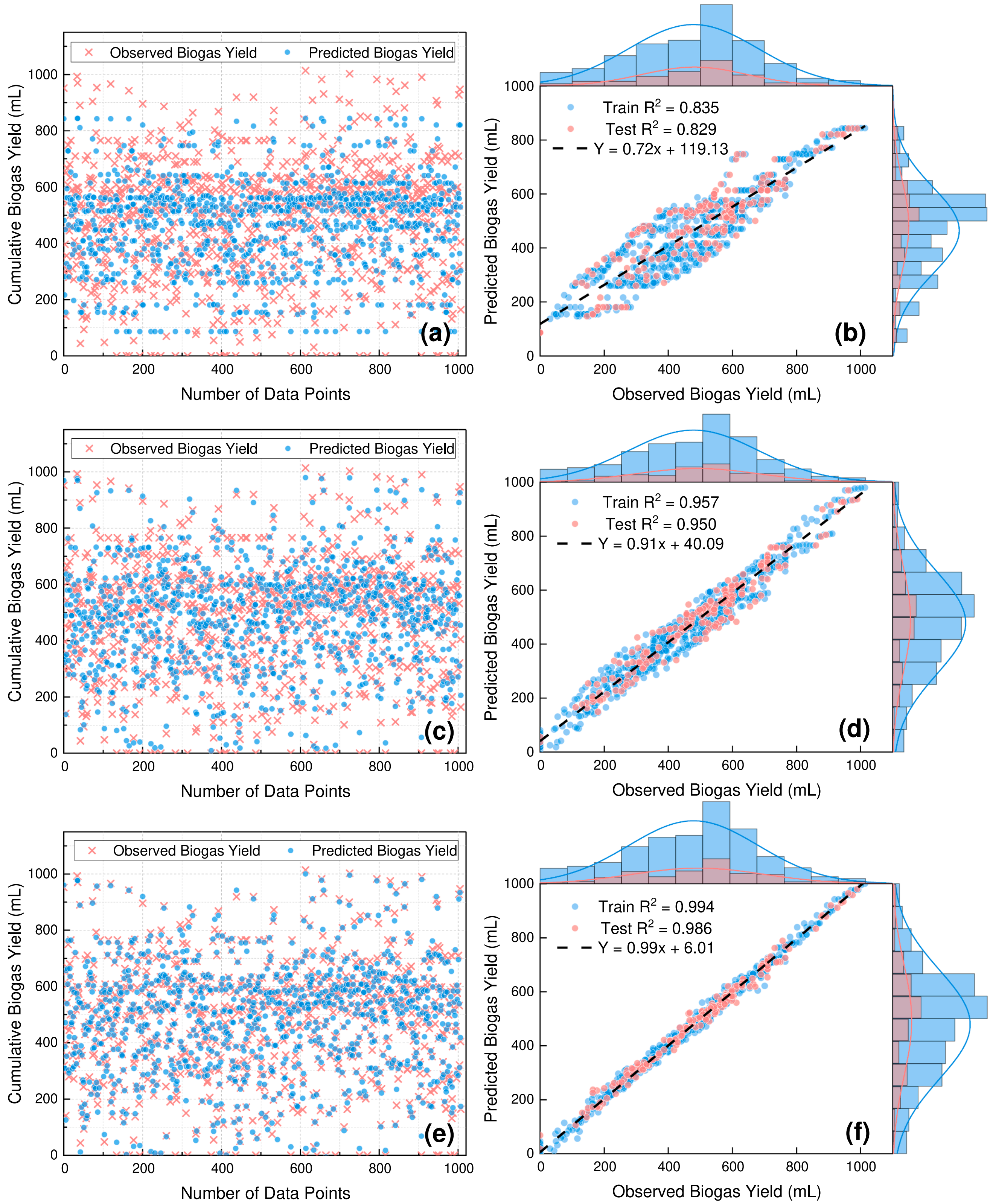

Fig. 1. Performance evaluation of machine learning models for predicting cumulative biogas yield (CBY). (a), (c), and (e) present actual versus predicted CBY for the AdaBoost, LGBM, and XGB models, respectively. (b), (d), and (f) show the corresponding correlation plots between observed and predicted CBY, including marginal histograms.

indicate the models' effectiveness in reflecting the underlying trends in the dataset, with LGBM and XGB demonstrating particularly high precision in forecasting biogas yields, as evidenced by their elevated R^2 values.

To gain a more nuanced understanding of each model's performance, the RMSE and MAE metrics provide additional insights. The RMSE values, which represent the standard deviation of prediction errors, are 88.79 for AdaBoost, 46.87 for LGBM, and 24.62 for XGB, indicating progressively better performance in minimizing large errors across the models. Similarly, the MAE values, i.e. 76.35, 35.78, and 16.40, respectively, reflect the average magnitude of errors. XGB, with the lowest error across both metrics, demonstrates superior accuracy in its predictions.

While all models demonstrate strong predictive capabilities for biogas yield, XGB stands out with the lowest error metrics, confirming its precision as the most accurate among the tested algorithms. LGBM offers a balanced combination of error minimization and computational efficiency. Although AdaBoost exhibits higher error metrics, it still achieves a commendable level of predictive accuracy. Overall, these results validate the effectiveness of ensemble learning methods in modelling complex phenomena such as biogas production.

3.1.2. Analysis of features importance

The analysis of input feature importance in predicting biogas yield was performed using the SHAP method, based on the XGB model, which demonstrated the highest predictive performance among the three evaluated ML models. As shown in Fig. 2a, TS % emerged as the most influential variable, accounting for 42 % of the total model importance. This underscores its pivotal role in AD, as higher TS concentrations generally enhance microbial activity and substrate availability, thereby improving biogas production efficiency [42,43]. The second most important factor was pH (28 %), reflecting its well-established influence on maintaining microbial community stability, particularly methanogens [44,45]. Microwave holding time accounted for 18 %, suggesting that prolonged exposure facilitates enhanced solubilization and hydrolysis processes, ultimately improving digestion efficiency.

Interestingly, microwave power was ranked as the least influential variable by SHAP, with only 12 % importance. This result appears to contrast with the experimental comparisons presented earlier (e.g., Runs 5 and 16), where changes in microwave power led to substantial differences in biogas yield. This discrepancy can be attributed to how SHAP evaluates feature importance in a global, nonlinear context. Rather than focusing on localised or extreme case effects, SHAP accounts for the average marginal contribution of each variable across all samples in the dataset. In the case of microwave power, its influence is highly context-dependent—it interacts non-linearly with other variables, such as holding time and TS %, and may exhibit threshold or saturation behaviour. Therefore, while microwave power can cause large differences in yield under specific conditions, its overall contribution appears smaller when averaged across the full experimental range.

The SHAP value plot (Fig. 2b) further illustrates the interactions among the key input variables. While higher TS % values consistently correlate with increased biogas yield, pH, and holding time exhibit more complex patterns, contributing positively or negatively depending on their interaction with other variables. In contrast, microwave power shows a diffuse distribution of SHAP values, with no consistent trend correlating power level with yield. This suggests that microwave power influences biogas production through more intricate mechanisms—potentially involving nonthermal effects—which are not linearly or uniformly captured across the dataset. A more detailed discussion of these nonthermal effects is provided in Section 3.3.

3.2. The RSM based model

The study addressed a complex modelling challenge involving multiple input variables and a single output metric. It was found that all four adjustable variables significantly affected the outcome. To illustrate how these input factors influenced the result, both two-dimensional (2D) contour plots and three-dimensional (3D) surface visualizations were employed using RSM. The software Design Expert was instrumental in developing equations that describe the relationships between the inputs and the output. Following data collection and experimental design, a detailed analysis was conducted to assess the impact of the input factors and construct a regression model. A comprehensive Analysis of Variance (ANOVA) was performed to determine the statistical significance of the variables and their interactions. This method effectively decomposes the overall variation in the output, attributing it to individual input factors and their combinations, thus revealing the comparative importance of each. It helps to identify which variables significantly influence the performance of the system. Table S4 presents the results of the ANOVA, providing a numerical understanding of the impact and interaction of the variables on system performance. This thorough statistical analysis led to the development of a response equation, as shown in Eq. (5).

$$\text{Cumulative Biogas Yield } (mL/gVS) = 608 + 58.17A + 31.67B$$

$$+116.16C - 130.37D - 2.72AB - 54.25AC - 85.87AD - 36.85BC - 4.15BD + 2.93CD - 30.52A^2 - 25.53B^2 + 28.77C^2 + 90.83D^2 \quad (5)$$

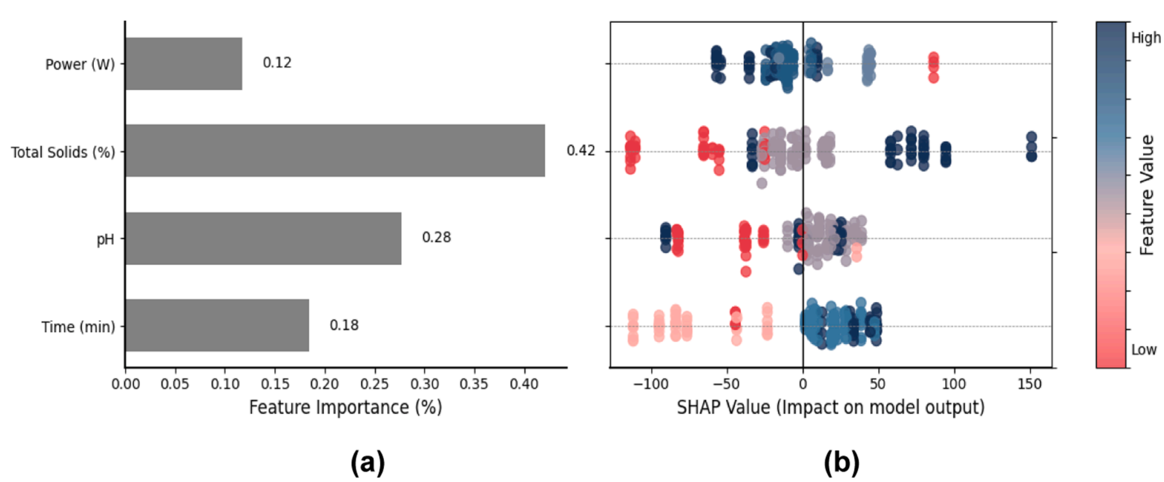

Fig. 2. Analysis of the importance of input features to output features: (a) Feature importance (%) for biogas; (b) SHAP values showing feature impact on biogas yield prediction.

Where: A is the holding time (min), B is the pH, C is the total solids content (TS %), and D is the microwave power (W).

3.2.1. Analysis of factor importance

The ANOVA results for biogas yield (Table S4) highlight the significance of various factors and their interactions. The model, with 14 degrees of freedom, shows a highly significant F-value of 28.05 ($p < 0.0001$), confirming its statistical robustness and indicating that the factors collectively influence biogas yield. Microwave power (D) exhibits the highest significance, with an F-value of 132.16 and a p-value of < 0.0001, suggesting a strong impact on biogas production within the linear statistical framework of ANOVA.

However, when compared with the SHAP analysis from the XGB model, a contrasting pattern emerges. SHAP identifies TS % as the most critical factor, contributing 42 % to the model's predictive accuracy. This difference stems from the fundamental methodologies of the two

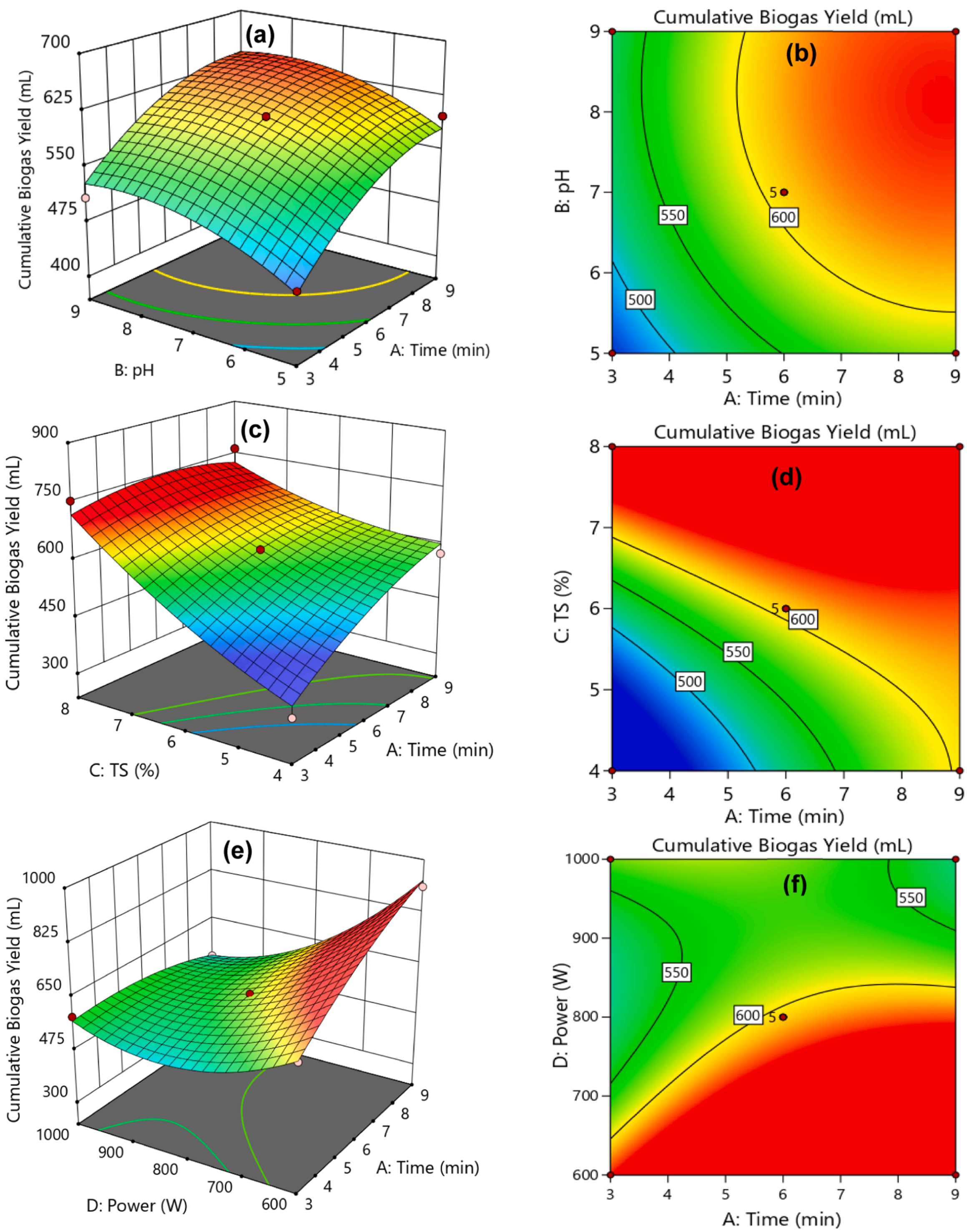

Fig. 3. Three-dimensional surface plots and two-dimensional contour plots for biogas production yield. (a) and (b) show the effects of time and pH; (c) and (d) present the impact of time and TS%; (e) and (f) illustrate the impact of time and microwave power. These plots identify the optimal operating conditions for maximizing biogas production..

approaches: while ANOVA assesses factor effects through linear relationships, SHAP captures complex, non-linear interactions within the AD process, providing a more nuanced view of variable importance.

Despite ANOVA emphasizing microwave power, TS % (C) also shows a significant F-value of 123.08 ($p < 0.0001$), reinforcing its pivotal role in biogas yield. The pronounced effect of microwave power in ANOVA may reflect its direct thermal influence, which linear models can readily detect. In contrast, the influence of TS % likely involves non-linear interactions and biological complexities, which are better captured by machine learning models like XGB. Similarly, pH (B) emerges as a key factor in both analyses. SHAP ranks pH as the second most influential variable (28 % importance), which aligns with its statistical significance

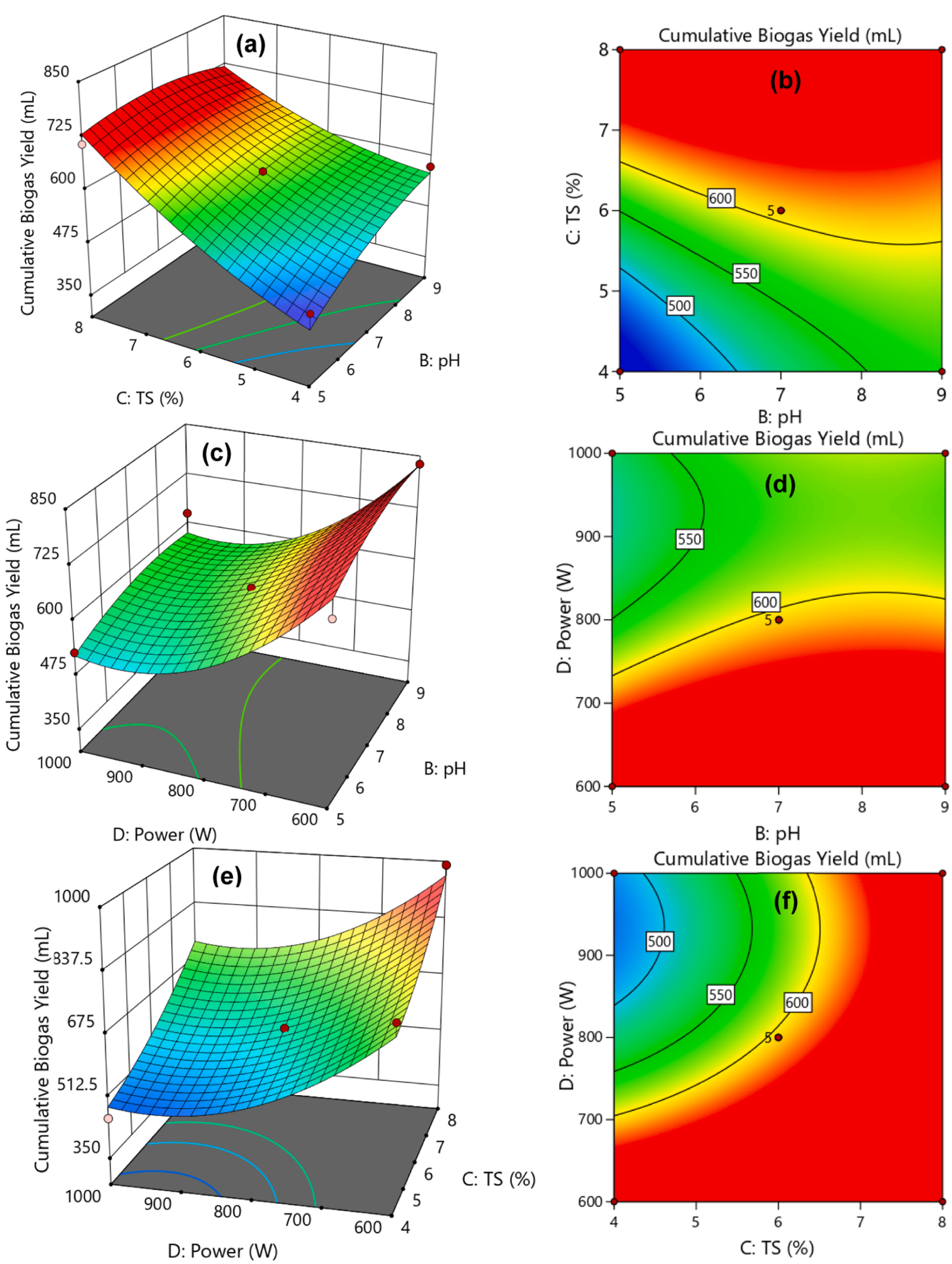

Fig. 4. Three-dimensional surface plots and two-dimensional contour plots for biogas production yield. (a) and (b) show the effects of holding time and microwave power; (c) and (d) present the impact of pretreatment temperature and microwave power; (e) and (f) illustrate the effects of pretreatment temperature and holding time.

in ANOVA ($F = 9.15$, $p = 0.0091$). This consistency underscores the critical role of pH in maintaining optimal conditions for microbial activity, highlighting its importance in both linear and non-linear analytical contexts.

The role of microwave power presents a more complex picture. While ANOVA identifies it as the dominant factor, SHAP assigns it a lower importance (12 %). This variation may be due to SHAP's ability to capture non-linear dependencies and the potential influence of non-thermal effects, which linear models like ANOVA do not fully reflect. The spread of SHAP values suggests that microwave power's effect on biogas yield is not uniform; instead, it appears to interact with other variables, such as holding time (A) and TS % (C). Notably, these factors also exhibit significant interaction effects in ANOVA (AC, AD) with p-values of 0.0097 and 0.0003, respectively. While SHAP interpretation of ML models has been increasingly applied in environmental modelling [46,47], few studies have directly compared it with traditional statistical methods like RSM in the context of anaerobic digestion.

This comparison illustrates the complementary strengths of ANOVA and SHAP. While ANOVA effectively identifies strong, direct relationships, such as the thermal effects of microwave power, SHAP reveals hidden, non-linear dynamics that better reflect the complex behaviour of biological systems like AD. For instance, the high SHAP value for TS % highlights its critical role in substrate availability, where increases do not always lead to proportional biogas yield due to microbial limitations or substrate saturation effects. Conversely, ANOVA may overstate the influence of microwave power because it does not account for these non-linear biological feedback mechanisms.

By integrating insights from both ANOVA and SHAP, it gains a more comprehensive understanding of the factors influencing biogas production. ANOVA provides clarity on linear, additive effects, while SHAP captures intricate non-linear interactions common in AD processes. To further evaluate the model's assumptions, a normal probability plot (Figure S3a) confirmed the normal distribution of residuals, while the residual versus run plot (Figure S3b) helped identify potential hidden factors influencing experimental outcomes.

3.2.2. *Factor interactions and optimal conditions*

Figs. 3 and 4 illustrate the interaction and influence of various input factors on biogas yield using a combination of 3D surface plots and 2D contour plots. In Fig. 3, the relationship between holding time and three key parameters, i.e. pH, TS %, and microwave power, is presented. In the holding time versus pH section (Fig. 3a-b), the graphical representations show a peak in biogas yield at a pH level close to neutral and an intermediate holding time. This suggests a non-linear response of biogas production to pH and time, with optimal production occurring when both factors are balanced. A reduction in yield is observed at lower pH values and extreme holding times, indicating that maintaining a neutral pH and moderate holding time is crucial for maximizing efficiency.

In the holding time versus TS % section (Fig. 3c–d), the plots show that biogas yield increases with TS % up to approximately 7 %, after which the yield levels off. The highest yield is observed at an intermediate holding time, confirming that both TS % and holding time must be optimized together [48]. Notably, the effect of TS % becomes more pronounced at longer holding times, indicating that higher substrate availability plays a key role in enhancing biogas production [49].

When examining the interaction between holding time and microwave power (Fig. 3e-f), the data suggest that biogas yield is maximized at moderate power levels, with an optimal holding time of around 6–7 min. Both excessive power and prolonged holding times result in diminished yields, pointing to a narrow range of conditions where microwave power is most effective. This highlights the importance of balancing energy input and processing time for optimal biogas generation.

In Fig. 4, the interaction between different pairs of parameters is analysed: pH and TS %, microwave power and pH, and microwave power and TS %. The pH versus TS % section (Fig. 4a-b) shows that the highest biogas yield is achieved at higher TS content combined with a neutral to slightly alkaline pH. Both lower pH levels and reduced TS % lead to lower yields, reinforcing the importance of maintaining optimal pH conditions alongside substrate concentration for effective microbial digestion [50].

In the power versus pH section (Fig. 4c-d), the plots show that a combination of moderate microwave power and neutral pH yields the highest biogas output. The non-linear trend observed indicates that both lower and higher power inputs are less effective when pH deviates from neutral, suggesting a synergistic effect between these two parameters. This reinforces the observation from Fig. 3 that both pH and microwave power must be optimized together to achieve maximum biogas production.

Lastly, in the power versus TS % section (Fig. 4e-f), the data suggest that the highest yields occur when microwave power is maintained at moderate levels while TS % is maximized. There is a clear trade-off between excessive power and high solids concentration, where yields begin to diminish beyond an optimal point. This indicates that substrate concentration and energy input must be carefully calibrated to avoid over-processing and inefficiencies.

Overall, these figures demonstrate that biogas yield is governed by a complex interaction of factors rather than being driven by any single parameter. Optimal production conditions are achieved by carefully balancing holding time, pH, TS %, and microwave power. The peaks in the 3D plots and the central regions of high yield in the contour plots clearly define the specific conditions required for optimal biogas generation. This analysis provides valuable insights for determining the best operational parameters in biogas production systems and can serve as a foundation for future experimental designs or for the development of predictive models to enhance process efficiency.

3.2.3. *Optimization through RSM*

In this study, RSM was employed to optimize the biogas production process. The primary goal was to maximize CBY, with key input variables identified as holding time (A), pH (B), TS % (C), and microwave power (D). These variables were investigated within the following ranges: holding time (3–9 min), pH (5–9), TS % (4–8 %), and microwave power (600–1000 W), as detailed in Table S5.

Based on the RSM optimization results, the predicted optimal conditions were determined as follows: 8.999 min holding time, pH of 6.923, 7.999 % TS, and 600 W microwave power. Under these conditions, the RSM predicted a CBY of 1020.484 mL/gVS. A validation experiment was conducted to verify these predicted values, and the observed biogas yield was 1013.8 mL/gVS. This observed result closely aligns with the predicted value, confirming the accuracy of the RSM model.

Furthermore, Figure S4 presents ramp plots generated during the desirability analysis. The desirability score, which ranges from 0 to 1, indicates the quality of the optimization, with higher values reflecting more favourable outcomes. In this study, the composite desirability score was 0.894, demonstrating a strong alignment between the optimized conditions and the biogas yield response. The ramp plots illustrate that each input factor, i.e. holding time, pH, TS, and microwave power, contributes significantly to maximizing the CBY when set to their respective optimal values.

The results of the RSM optimization and validation test confirm that the interplay of operational parameters (i.e. holding time, pH, TS, and microwave power) can be effectively fine-tuned to achieve optimal biogas production. The close agreement between the predicted and observed yields underscores the reliability of RSM as a tool for optimizing AD processes, providing valuable insights into the key factors that influence biogas yield.

3.3. *Nonthermal effects of microwave pretreatment*

MP is widely recognized for its thermal effects, which enhance sludge solubilization and microbial hydrolysis. However, our findings suggest that microwave irradiation may induce additional nonthermal effects, such as electromagnetic interactions with microbial cell membranes and EPS, as well as enhanced organic matter solubilization beyond what conventional heating achieves. To isolate these nonthermal effects, this study compares biogas yield and sludge structural integrity across four experimental conditions, all reaching the same final temperature of 85 °C, while maintaining pH = 7 and TS % = 8 in sludge samples. The experimental conditions include No Pretreatment (Original), CH to assess pure thermal effects without microwave exposure, Microwave (MW) 600 W to evaluate the effects of low microwave power and MW 1000 W to examine the impact of higher microwave power. By maintaining identical temperature conditions across all treatments, any observed differences in biogas yield and sludge structure can be attributed to microwave nonthermal effects rather than heat alone.

3.3.1. *Biogas yield and improvement in sludge digestibility*

The biogas yield profiles for the four experimental conditions—Original, Conventional Heating (CH 85 °C), Microwave 600 W (MW 600 85 °C), and Microwave 1000 W (MW 1000 85 °C)—are presented in Fig. 5. The results indicate distinct differences in biogas production trends, highlighting the effects of thermal and microwave-specific nonthermal influences.

Throughout the digestion period, all pretreatment methods significantly enhanced biogas production compared to the Original condition. The CH 85 °C treatment increased CBY by 37.3 % (from 615.3 mL/gVS to 844.8 mL/gVS), while MW 600 85 °C and MW 1000 85 °C resulted in even greater improvements of 62.8 % (1002.3 mL/gVS) and 56.1 % (960.4 mL/gVS), respectively. These results highlight the effectiveness of thermal and microwave-assisted pretreatment in enhancing biogas yield, demonstrating that pretreatment significantly improves sludge digestibility compared to untreated sludge.

When comparing CH with MP, MW 600 W 85 °C produced 18.6 % more biogas than CH 85 °C, while MW 1000 W 85 °C achieved a 13.7 % increase over CH 85 °C. These differences suggest that MP offers additional benefits beyond CH, likely due to both thermal and nonthermal effects. Between the two microwave power levels, MW 600 W outperformed MW 1000 W by 4.4 %, despite both reaching the same target temperature. This indicates that although both MW 600 W and MW 1000 W reached the same final temperature, the lower microwave power (600 W) required a longer heating time, leading to prolonged microwave exposure. These findings are consistent with Park et al. [51], who reported that moderate microwave power enhances solubilization more effectively than high power under the same temperature conditions, and build upon the work of Alhraishawi et al. [52], who observed diminishing returns at excessive power levels due to microbial inhibition. Unlike previous studies that focused primarily on thermal effects, our results isolate and quantify the added benefit of nonthermal effects by maintaining consistent final temperatures across treatments.

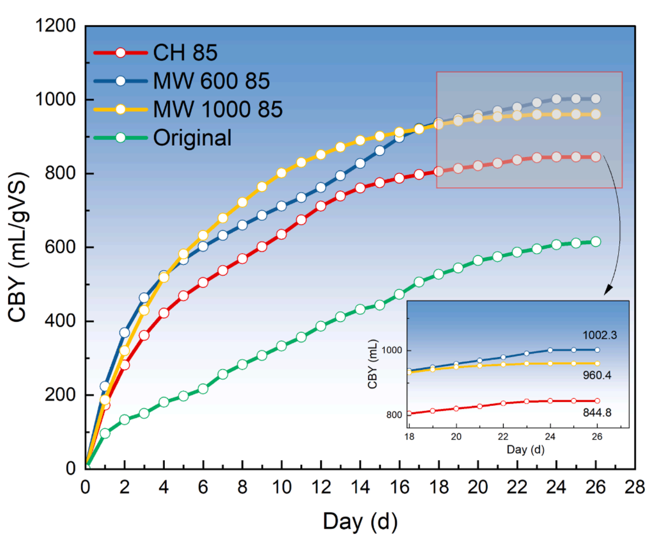

Fig. 5. Cumulative biogas yield (CBY, mL/g VS) over 26 days under four conditions: untreated sludge, conventional heating at 85 °C (CH 85), microwave pretreatment at 600 W to 85 °C (MW 600 85), and microwave pretreatment at 1000 W to 85 °C (MW 1000 85). The inset provides a magnified view of days 18–26.

Additionally, based on the relationship between wavelength and frequency, lower microwave power corresponds to a longer wavelength, allowing electromagnetic waves to penetrate deeper into the sludge matrix. This deeper penetration may have enhanced cell membrane permeability and organic matter solubilization, improving overall biogas production. These observations align with previous studies suggesting that moderate microwave power enhances microbial accessibility to substrates through structural modifications, while excessive microwave intensity may lead to detrimental effects on microbial viability.

3.3.2. *Structural integrity assessment by fluorescence microscopy*

To further investigate the structural modifications induced by different pretreatment methods, fluorescence microscopy was employed to analyse changes in EPS and microbial structure. FITC (green) staining was used to visualize proteins, while Calcofluor White (blue) staining highlighted polysaccharides, providing insights into cell integrity and EPS degradation.

The fluorescence microscopy images (Fig. 6) reveal distinct differences in EPS structure and microbial integrity among the experimental conditions. The Original (untreated) sample exhibits a dense and well-preserved EPS network, as indicated by the strong green (protein) and blue (polysaccharide) fluorescence signals, with proteins forming continuous, elongated chains and a uniformly distributed polysaccharide matrix. In contrast, the CH 85 °C treated sample shows a more loosely structured EPS network. The protein distribution appears more fragmented, with fewer long-chain structures and a predominance of smaller, cut pieces, suggesting partial EPS degradation and disruption of microbial interactions. This structural loosening is likely due to thermal solubilization effects, which facilitate EPS breakdown while maintaining overall microbial integrity.

Microwave treated samples exhibit more pronounced structural modifications, reinforcing the hypothesis that non-thermal effects influence microbial integrity. The MW 600 W 85 °C sample displays a more dispersed EPS structure, characterized by increased microbial cell permeability and loosening of the polysaccharide matrix, indicative of enhanced sludge disintegration. These modifications likely improve substrate accessibility, contributing to the higher biogas yield observed in MW 600 W pretreatment. In contrast, the MW 1000 W 85 °C sample exhibits a more fragmented EPS structure with localized disruptions in fluorescence distribution, suggesting that excessive microwave power may lead to over-disintegration. This over-fragmentation could potentially compromise microbial viability and trigger the release of inhibitory compounds, which may explain the slight reduction in biogas yield compared to MW 600 W 85 °C.

These structural observations align with Yu et al. [53], who demonstrated that microwave pretreatment leads to EPS disruption and increased microbial permeability. Building on this, our study introduces a novel quantitative layer by using ImageJ software to analyse particle distribution, fluorescence intensity, and EPS coverage. This approach not only confirms the visual trends observed in fluorescence microscopy (Table S6) but also links these structural shifts directly to biogas output under controlled thermal conditions, thereby bridging a key gap in mechanistic understanding.

For protein (FITC, green), MW 600 W 85 °C exhibited a high total protein area (13,347,673) and particle count (96,673), indicating

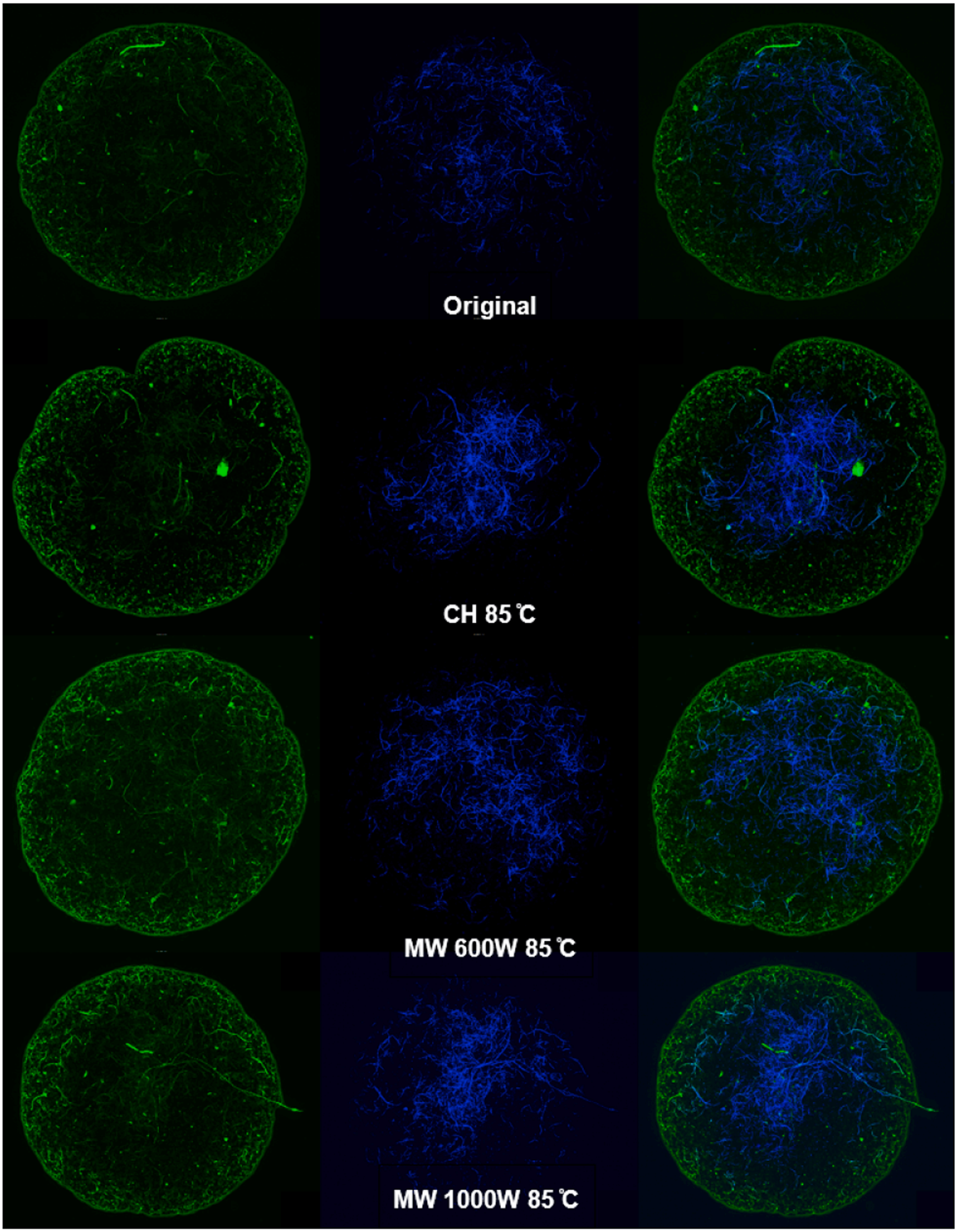

Fig. 6. Fluorescence microscopy images of sludge samples under different pretreatment conditions. Proteins are stained with FITC (green), and polysaccharides are stained with Calcofluor White (blue).

enhanced protein dispersion and EPS disintegration. However, MW 1000 W 85 °C had a slightly higher total area (13,597,443.7) but smaller average particle size (127.355 compared to 138.07 for MW 600 W 85 °C), suggesting over-fragmentation and potential microbial stress. CH 85 °C had a lower total protein area (9752,005.22) and particle count (62,392) than MP samples, reflecting moderate EPS degradation due to thermal solubilization. For polysaccharides (Calcofluor White, blue), MW 600 W 85 °C resulted in the highest total polysaccharide area (8394,481.8) and particle count (13,024), reinforcing its role in optimizing substrate accessibility. In contrast, MW 1000 W 85 °C exhibited a slight reduction in total area (8065,280.73) and particle count (12,905), indicating possible EPS over-degradation at higher microwave power. CH treated sludge showed the lowest polysaccharide particle count (12,038) and total area (4745,186.09), suggesting thermal breakdown of EPS without additional structural enhancement.

Compared to the Original sample, which maintained a dense EPS network with a total protein area of 6848,148.5 and polysaccharide area of 5108,616.71, CH treatment at 85 °C led to a reduction in total EPS area and particle count, confirming EPS degradation due to thermal solubilization. Meanwhile, MW 600 W 85 °C exhibited the most extensive EPS dispersion, reinforcing its role in enhancing microbial accessibility and sludge disintegration. In contrast, although MW 1000 W 85 °C still facilitated significant EPS breakdown, its lower EPS coverage and increased fragmentation suggest that excessive microwave power may cause microbial stress and over-disintegration.

While microwave pretreatment clearly alters microbial and EPS structure, it is essential to contextualize these changes within the broader framework of all process parameters. For example, holding time directly affects the degree of thermal and nonthermal exposure; longer holding times at moderate power can lead to more uniform disruption of EPS, whereas short bursts at high power may cause local overheating and stress. Similarly, TS % content modulates microbial accessibility—higher TS concentrations increase substrate availability but may also lead to diffusion limitations if the sludge becomes overly dense. These variables are not independent; their interactions often shape the observed outcomes. For instance, fluorescence signals from MW 600 W could reflect not only optimal microwave intensity but also an effective combination of exposure duration and substrate composition. Therefore, attributing changes solely to microwave intensity may oversimplify a more complex synergy. A balanced interpretation should consider how holding time, TS %, and pH interact with microwave energy to influence structural changes, microbial viability, and ultimately biogas production.

These quantitative results further support the previous discussion on the discrepancy between ML and RSM factor importance rankings. In previous section, ML identified TS % as the most influential factor, whereas RSM emphasized microwave power. This variation was attributed to ML's ability to capture non-linear relationships, particularly the complex interactions within microwave pretreatment effects. The fluorescence microscopy and ImageJ analysis confirm that microwave pretreatment does not have a simple linear effect—while moderate microwave exposure enhances sludge disintegration and microbial access to substrates, excessive intensity results in unintended structural damage and potential microbial stress. This aligns with the non-linear correlation captured by ML, where increasing microwave power does not always proportionally enhance biogas yield. Therefore, these findings reinforce the need to consider non-linear factor interactions when optimizing anaerobic digestion efficiency, as captured by ML-based analysis.

Compared to earlier research, which often either focused on microwave pretreatment [54,55] or ML optimization of anaerobic digestion [11,56], this study uniquely integrates both in a unified experimental and modelling framework. By validating ML-predicted trends with mechanistic insights (i.e., structural EPS changes), the work bridges empirical and computational domains. This integration helps overcome limitations noted in previous work, i.e., the lack of interpretability in ML predictions and the neglect of nonthermal microwave effects.

4. Energy and economic evaluation

While MP currently consumes more energy than traditional thermal methods, it holds significant long-term potential for cost and energy savings in the AD process. Microwave technology provides rapid, uniform heating, which enhances the breakdown of organic substrates, leading to higher biogas yields and shorter processing times [57,58]. However, to fully realize these benefits, continuous optimization is necessary to improve its energy efficiency and reduce operational costs.

4.1. Advancements and economic outlook

Historically, microwave technology was prohibitively expensive for industrial applications, but significant advancements have driven down costs over the past few decades. In the late 20th century, the high cost of microwave systems limited their use to specialized industrial processes [59]. However, innovations in manufacturing, semiconductor technology, and energy efficiency have led to a reduction in the cost of microwave systems by >80 % since the 1990s [60]. For example, the widespread adoption of microwave ovens in households has demonstrated the scalability and affordability of microwave technology, suggesting that with further advancements, its use in industrial scale AD could become more economically feasible [61].

The trend of cost reductions is expected to continue as new microwave technologies emerge, particularly those designed for energy recovery and real-time process optimization. As these technologies improve, the cost and energy barriers to adopting MP in biogas production will decrease, making it a more viable option for large-scale applications in waste-to-energy systems.

4.2. Policy incentives for AD and biogas

Governments worldwide are increasingly implementing policies to encourage environmentally friendly technologies, particularly those that reduce greenhouse gas emissions and encourage renewable energy. AD, recognized as a crucial technology in the transition to a low-carbon economy [62–64], has been targeted by various policies offering financial incentives and subsidies to support its adoption.

Table 2 summarizes key policies related to AD and biogas production across several regions, highlighting the incentives available to promote cleaner energy solutions.

These policies reflect the global recognition of AD as a vital component of waste management and renewable energy production. In regions such as the European Union and the UK, financial support for developing biogas facilities is readily available, reducing the economic barriers for industries to adopt technologies like MP. These incentives can offset the initial costs of upgrading biogas facilities with advanced pretreatment methods, making it easier for companies to justify investments in innovative technologies.

4.3. Energy optimization and scalability

Enhancing the energy efficiency and cost-effectiveness of MP in AD requires integrating ML with RSM. This study demonstrated that ML, particularly XGB, captures non-linear process interactions, while RSM determines optimal conditions, reducing operational inefficiencies and energy waste. By identifying TS %, and microwave power as key parameters, ML-RSM optimization enables targeted energy reduction without compromising biogas yield. This study found that moderate microwave power (600 W) maximized efficiency, preventing unnecessary energy input while maintaining high biogas yields. Such a data-driven approach improves process efficiency and cost-effectiveness, reinforcing MP as a sustainable AD enhancement strategy.

As MP technology advances, automated ML-based control systems

Table 2
Global Policy Incentives and Goals for Anaerobic Digestion and Biogas Production.

Country/ Region	Key Policies for Anaerobic Digestion	Incentives/Goals	Reference
Australia	National Waste Policy Action Plan	• Grants for waste-to-energy projects • Divert 80 % of organic waste by 2030 • Reduce methane emissions	[65]
China	13th Five-Year Plan for Bioenergy Development	• 2.5 billion RMB subsidies • Promote biogas production • Reduce agricultural waste	[66]
European Union	Renewable Energy Directive	• 32 % renewable energy by 2030 • Feed-in tariffs & capital grants • Reduce methane & fossil fuel reliance	[67]
United Kingdom	Anaerobic Digestion Strategy	• Renewable Heat Incentive • Contracts for Difference • Support net-zero by 2050	[68]
United States	Renewable Fuel Standard	• Mandates renewable fuels • Tax credits & subsidies for RNG • Cut GHG emissions & boost energy security	[69]

offer real-time process optimization, dynamically adjusting parameters based on predicted biogas yields. This would minimize energy consumption, reduce manual intervention, and eliminate costly trial-and-error experiments, making MP more economically viable at scale. The scalability of ML-RSM integration has significant implications for industrial-scale AD applications. As industries move toward automated process control, continuous data-driven optimization will improve energy efficiency and cost savings. Meeting global climate targets, such as 2050 net-zero goals [70,71], requires widespread adoption of energy-efficient biogas technologies. Optimizing MP with real-time ML-driven frameworks will further enhance process sustainability and scalability, making it a viable solution for waste-to-energy applications.

4.4. Innovation in bioenergy technologies

To evaluate the energy efficiency of microwave and conventional thermal pretreatment, energy input was calculated based on the specific heating approach used.

For conventional thermal heating, the energy required to raise the temperature of sludge from ambient (25 °C) to 85 °C was estimated using Eq. (6).

$$Q = \frac{m \cdot C_p \cdot \Delta T}{\eta} \quad (6)$$

Where: Q is the energy input (kJ); m is the sludge mass (kg, approximated equal to volume in litres due to near-water density); C_p is specific heat capacity of sludge (≈4.18 kJ/kg· °C, approximated as water); ΔT is temperature rise (60 °C) and η is heating efficiency.

For microwave pretreatment, energy input was calculated using Eq. (7):

$$Q = \frac{P \cdot t}{\eta} \quad (7)$$

Where, P is microwave power (kW); t is heating time (hours); η is heating efficiency; and Q is energy input, converted from kWh to MJ.

All experiments were conducted using 400 mL of sludge per batch. Energy values were scaled to per litre (MJ/L) for comparison. Additionally, energy input was normalized against biogas yield (cumulative biogas yield, CBY) to obtain energy input per litre of biogas produced (MJ/L biogas), as shown in Table 3.

The comparative energy input analysis reveals that CH 85 °C required 0.42 MJ/L of sludge, while microwave pretreatment at 600 W and 1000 W consumed 0.72 MJ/L and 0.70 MJ/L, respectively. Although microwave pretreatment entails higher initial energy input, it also delivers higher cumulative biogas yield, particularly at 600 W. When normalized by biogas output, the energy input per litre of biogas produced is 0.50 MJ/L for CH, 0.72 MJ/L for MW 600 W, and 0.73 MJ/L for MW 1000 W. Despite the higher input, MW 600 W still demonstrates a favourable energy-to-yield trade-off, outperforming CH in net energy recovery. Compared to MW 1000 W, MW 600 W also shows better efficiency, indicating that moderate power levels achieve optimal biogas enhancement without unnecessary energy expenditure.

However, the current experimental setup has several limitations. The study was conducted at laboratory scale, using 400 mL of sludge per batch and a domestic microwave unit. Such setups typically suffer from lower energy transfer efficiency and a lack of thermal recovery mechanisms. Moreover, batch-based microwave heating is less controlled than continuous industrial systems, potentially overstating the real energy input required. As emphasized in earlier literature [7,58], industrial-scale microwave systems benefit from higher conversion efficiency, better heat distribution, and potential integration with waste heat recovery or pulsed power systems, which could significantly reduce energy demands [72]. Therefore, the current results should be interpreted as a conservative scenario, and future work at pilot or industrial scale is essential to fully assess the net energy and economic benefits of microwave pretreatment in real-world anaerobic digestion applications.

5. Conclusions

This study developed a synergistic framework that integrates statistical optimization through RSM with advanced ML models to enhance biogas production from microwave-pretreated waste-activated sludge. The results demonstrated that microwave pretreatment at moderate intensity (600 W, 85 °C) achieved the highest cumulative biogas yield (1002.3 mL/gVS), outperforming both conventional heating (844.8 mL/gVS) and untreated sludge, thereby confirming that pretreatment significantly improves sludge digestibility. RSM optimization further predicted an optimal yield of 1020.5 mL/gVS under conditions of 9 min holding time, pH 6.9, 8 % TS, and 600 W microwave power, which was closely validated by experimental results (1013.8 mL/gVS).

The predictive capability of ML was also evident, with XGBoost achieving the highest accuracy (R^2 = 0.992), followed by LGBM and AdaBoost. SHAP-based feature importance analysis revealed that TS % was the dominant factor, while RSM emphasized microwave power, underscoring the complementary strengths of linear statistical and nonlinear ML approaches. Fluorescence microscopy and ImageJ analysis provided mechanistic confirmation of microwave-induced nonthermal effects, particularly under moderate power conditions, where enhanced

Table 3
Energy input and biogas yield comparison.

Condition	Energy Input (MJ/L sludge)	CBY (mL/g VS)	Energy Input per Litre Biogas (MJ/L)
Original	0.00	615.30	0.00
CH 85 °C	0.42	844.80	0.50
MW 600 W 85 °C	0.72	1002.30	0.72
MW 1000 W 85 °C	0.70	960.40	0.73

EPS disintegration and microbial accessibility were observed without the over-fragmentation associated with excessive power levels. By bridging computational predictions with mechanistic validation, this work delivers both predictive accuracy and biological insight into microwave-assisted anaerobic digestion.

Looking forward, future research should scale this framework from laboratory to pilot and industrial systems, particularly under continuous-flow conditions that incorporate energy recovery mechanisms. Expanding the modelling framework to integrate multi-omics data, including microbial, metabolomic, and antibiotic resistance gene profiles, would further enhance mechanistic understanding. In addition, the development of real-time ML-based control systems capable of dynamically adjusting pretreatment and digestion parameters could optimize energy efficiency in practical applications. Finally, techno-economic and life-cycle assessments are needed to evaluate the long-term sustainability and viability of microwave pretreatment at scale.

Overall, this study establishes a novel integrative approach that combines statistical, computational, and mechanistic perspectives to advance the optimization of anaerobic digestion. The findings contribute to both the scientific understanding and the practical application of microwave pretreatment, paving the way for more energy-efficient and sustainable sludge-to-biogas systems.

CRediT authorship contribution statement

Yuxuan Li: Writing – review & editing, Writing – original draft, Visualization, Validation, Methodology, Investigation, Formal analysis, Data curation, Conceptualization. **Mahuizi Lu:** Writing – review & editing, Visualization, Validation, Software, Resources, Data curation. **Luiza C. Campos:** Writing – review & editing, Supervision, Resources, Project administration. **Shikun Cheng:** Writing – review & editing. **Zifu Li:** Writing – review & editing. **Yukun Hu:** Writing – review & editing, Supervision, Software, Resources, Project administration, Methodology, Conceptualization.

Declaration of competing interest

The authors declare that they have no known competing financial interests or personal relationships that could have appeared to influence the work reported in this paper.

Supplementary materials

Supplementary material associated with this article can be found, in the online version, at doi:10.1016/j.nexus.2025.100583.

Data availability

Data will be made available on request.

References

[1] J. Sun, Y. Xu, S. Nairat, J. Zhou, Z. He, Prediction of biogas production in anaerobic digestion of a full-scale wastewater treatment plant using ensembled machine learning models, Water. Environ. Res. 95 (2023), https://doi.org/10.1002/wer.10893.

[2] R. Gupta, L. Zhang, J. Hou, Z. Zhang, H. Liu, S. You, et al., Review of explainable machine learning for anaerobic digestion, Bioresour. Technol. 369 (2023) 128468, https://doi.org/10.1016/j.biortech.2022.128468.

[3] M.I. Alfa, H.I. Owamah, A.O. Onokwai, S. Gopikumar, S.O. Oyebisi, S.S. Kumar, et al., Evaluation of biogas yield and kinetics from the anaerobic co-digestion of cow dung and horse dung: a strategy for sustainable management of livestock manure, Energy Ecol. Environ. 6 (2021) 425–434, https://doi.org/10.1007/s40974-020-00203-0.

[4] A. Elsayed, F.L. Kakar, A. Marcus, A. AlSayed, M.S. Zagloul, C. Muller, et al., Application of additives for anaerobic digestion intensification: a comprehensive review on improving biogas production and methane yield, Appl. Energy 381 (2025) 125202, https://doi.org/10.1016/j.apenergy.2024.125202.

[5] K. Jothibasu, I. Muniraj, T. Jayakumar, B. Ray, D.W. Dhar, S. Karthikeyan, et al., Impact of microalgal cell wall biology on downstream processing and nutrient removal for fuels and value-added products, Biochem. Eng. J. 187 (2022) 108642, https://doi.org/10.1016/j.bej.2022.108642.

[6] A.V. Agrawal, P.K. Chaudhari, P. Ghosh, Effect of microwave treatment on maximizing biogas yield for anaerobic co-digestion of fruit and vegetable waste and anaerobic sludge, BioMass Convers. Biorefin. (2023), https://doi.org/10.1007/s13399-023-04114-y.

[7] Y. Li, L.C. Campos, Y. Hu, Microwave pretreatment of wastewater sludge technology—a scientometric-based review, Environ. Sci. Pollut. Res. 31 (2024) 26432–26451, https://doi.org/10.1007/s11356-024-32931-9.

[8] S. Astals, M. Esteban-Gutiérrez, T. Fernández-Arévalo, E. Aymerich, J.L. García-Heras, J. Mata-Alvarez, Anaerobic digestion of seven different sewage sludges: a biodegradability and modelling study, Water. Res. 47 (2013) 6033–6043, https://doi.org/10.1016/J.WATRES.2013.07.019.

[9] L. Wang, F. Long, W. Liao, H. Liu, Prediction of anaerobic digestion performance and identification of critical operational parameters using machine learning algorithms, Bioresour. Technol. 298 (2020) 122495, https://doi.org/10.1016/j.biortech.2019.122495.

[10] Y. Wang, T. Huntington, C.D. Scown, Tree-based automated machine learning to predict biogas production for Anaerobic Co-digestion of organic waste, ACS. Sustain. Chem. Eng. 9 (2021) 12990–13000, https://doi.org/10.1021/acssuschemeng.1c04612.

[11] O. Yildirim, B. Ozkaya, Prediction of biogas production of industrial scale anaerobic digestion plant by machine learning algorithms, Chemosphere 335 (2023) 138976, https://doi.org/10.1016/j.chemosphere.2023.138976.

[12] H. Rutland, J. You, H. Liu, L. Bull, D. Reynolds, A systematic review of machine-learning solutions in Anaerobic digestion, Bioengineering 10 (2023) 1410, https://doi.org/10.3390/bioengineering10121410.

[13] Y. Li, M. Lu, L.C. Campos, Y. Hu, Predicting biogas yield after microwave pretreatment using artificial neural network models: performance evaluation and method comparison, ACS. ES. T. Eng. (2024), https://doi.org/10.1021/acsestengg.4c00276.

[14] M.O. Okwu, O.D. Samuel, D.R.E. Ewim, Z. Huan, Estimation of biogas yields produced from combination of waste by implementing response surface methodology (RSM) and adaptive neuro-fuzzy inference system (ANFIS), Int. J. Energy Environ. Eng. 12 (2021) 353–363, https://doi.org/10.1007/s40095-021-00381-5.

[15] American Public Health Association AWWAWEF, Standard Methods for the Examination of Water and Wastewater, 21st ed., American Public Health Association, 2005.

[16] F. Huang, H. Liu, J. Wen, C. Zhao, L. Dong, H. Liu, Underestimated humic acids release and influence on anaerobic digestion during sludge thermal hydrolysis, Water. Res. 201 (2021) 117310, https://doi.org/10.1016/j.watres.2021.117310.

[17] A. Serrano, J.A. Siles, M.A. Martín, A.F. Chica, F.S. Estévez-Pastor, E. Toro-Baptista, Improvement of anaerobic digestion of sewage sludge through microwave pre-treatment, J. Environ. Manag. 177 (2016) 231–239, https://doi.org/10.1016/j.jenvman.2016.03.048.

[18] R. Uma Rani, S. Adish Kumar, S. Kaliappan, I. Yeom, J. Rajesh Banu, Impacts of microwave pretreatments on the semi-continuous anaerobic digestion of dairy waste activated sludge, Waste Manage 33 (2013) 1119–1127, https://doi.org/10.1016/j.wasman.2013.01.016.

[19] H.I. Owamah, S.C. Ikpeseni, M.I. Alfa, S.O. Oyebisi, S. Gopikumar, O. David Samuel, et al., Influence of inoculum/substrate ratio on biogas yield and kinetics from the anaerobic co-digestion of food waste and maize husk, Environ. Nanotechnol. Monit. Manag. 16 (2021) 100558, https://doi.org/10.1016/j.enmm.2021.100558.

[20] S. Kolbl, A. Paloczi, J. Panjan, B. Stres, Addressing case specific biogas plant tasks: industry oriented methane yields derived from 5L Automatic Methane Potential Test Systems in batch or semi-continuous tests using realistic inocula, substrate particle sizes and organic loading, Bioresour. Technol. 153 (2014) 180–188, https://doi.org/10.1016/j.biortech.2013.12.010.

[21] S. Bellaton, S. Guérin, N. Pautremat, J. Bernier, M. Muller, S. Motellet, et al., Early assessment of a rapid alternative method for the estimation of the biomethane potential of sewage sludge, Bioresour. Technol. 206 (2016) 279–284, https://doi.org/10.1016/j.biortech.2016.01.139.

[22] J.V. Oliveira, M.M. Alves, J.C. Costa, Design of experiments to assess pre-treatment and co-digestion strategies that optimize biogas production from macroalgae Gracilaria vermiculophylla, Bioresour. Technol. 162 (2014) 323–330, https://doi.org/10.1016/J.BIORTECH.2014.03.155.

[23] K.O. Olatunji, D.M. Madyira, N.A. Ahmed, S.O. Jekayinfa, O. Ogunkunle, Modelling the effects of particle size pretreatment method on biogas yield of groundnut shells, Waste Manag. Res.: J. Sustain. Circ. Econ. 40 (2022) 1176–1188, https://doi.org/10.1177/0734242X211073852.

[24] D. Sun, S. Guo, N. Ma, G. Wang, C. Ma, J. Hao, et al., Sewage sludge pretreatment by microwave irradiation combined with activated carbon fibre at alkaline pH for anaerobic digestion, Water. Sci. Technol. 73 (2016) 2882–2887, https://doi.org/10.2166/wst.2016.149.

[25] B. Aylin Alagöz, O. Yenigün, A. Erdinçler, Enhancement of anaerobic digestion efficiency of wastewater sludge and olive waste: synergistic effect of co-digestion and ultrasonic/microwave sludge pre-treatment, Waste Manage 46 (2015) 182–188, https://doi.org/10.1016/J.WASMAN.2015.08.020.

[26] F. Passos, M. Hernández-Mariné, J. García, I. Ferrer, Long-term anaerobic digestion of microalgae grown in HRAP for wastewater treatment. Effect of microwave pretreatment, Water. Res. 49 (2014) 351–359, https://doi.org/10.1016/J.WATRES.2013.10.013.

[27] S.S. Djimtoingar, N.S.A. Derkyi, F.A. Kuranchie, J.K. Yankyera, A review of response surface methodology for biogas process optimization, Cogent. Eng. 9 (2022), https://doi.org/10.1080/23311916.2022.2115283.

[28] Okwu M.O., Tartibu L.K., Samuel O.D., Omoregbee H.O., Ivbanikaro A.E. Predictive ability of response surface methodology (RSM) and artificial neural network (ANN) to approximate biogas yield in a modular biodigester, 2021, p. 202–15. 10.1007/978-3-030-85030-2_17.

[29] Y. Zhan, J. Zhu, Response surface methodology and artificial neural network-genetic algorithm for modeling and optimization of bioenergy production from biochar-improved anaerobic digestion, Appl. Energy 355 (2024) 122336, https://doi.org/10.1016/J.APENERGY.2023.122336.

[30] N. Ferreira, T. Viana, B. Henriques, D.S. Tavares, J. Jacinto, J. Colónia, et al., Application of response surface methodology and box–behnken design for the optimization of mercury removal by Ulva sp, J. Hazard. Mater. 445 (2023) 130405, https://doi.org/10.1016/j.jhazmat.2022.130405.

[31] M. Safari, R. Abdi, M. Adl, J. Kafashan, Optimization of biogas productivity in lab-scale by response surface methodology, Renew. Energy 118 (2018) 368–375, https://doi.org/10.1016/j.renene.2017.11.025.

[32] M.S. Shehu, Z. Abdul Manan, S.R Wan Alwi, Optimization of thermo-alkaline disintegration of sewage sludge for enhanced biogas yield, Bioresour. Technol. 114 (2012) 69–74, https://doi.org/10.1016/J.BIORTECH.2012.02.135.

[33] F. Wang, Z. Li, F. He, R. Wang, W. Yu, F. Nie, Feature learning viewpoint of adaboost and a new algorithm, IEEe Access. 7 (2019) 149890–149899, https://doi.org/10.1109/ACCESS.2019.2947359.

[34] K.A. Shukla, G. Chettiar, A. Choudhary, A. Thakur, S. Kumar, Integrating comparison of malware detection classification using LGBM and XGB machine learning algorithms, in: 2022 IEEE International Conference on Blockchain and Distributed Systems Security (ICBDS), IEEE, 2022, pp. 1–7, https://doi.org/10.1109/ICBDS53701.2022.9935976.

[35] P. Trizoglou, X. Liu, Z. Lin, Fault detection by an ensemble framework of Extreme Gradient Boosting (XGBoost) in the operation of offshore wind turbines, Renew. Energy 179 (2021) 945–962, https://doi.org/10.1016/j.renene.2021.07.085.

[36] D. Chicco, M.J. Warrens, G. Jurman, The coefficient of determination R-squared is more informative than SMAPE, MAE, MAPE, MSE and RMSE in regression analysis evaluation, PeerJ. Comput. Sci. 7 (2021) e623, https://doi.org/10.7717/peerj-cs.623.

[37] D.S.K. Karunasingha, Root mean square error or mean absolute error? Use their ratio as well, Inf. Sci. 585 (2022) 609–629, https://doi.org/10.1016/J.INS.2021.11.036.

[38] Rajawat A.S., Mohammed O., Shaw R.N., Ghosh A. Renewable energy system for industrial internet of things model using fusion-AI. Applications of AI and IOT in Renewable energy 2022:107–28. 10.1016/B978-0-323-91699-8.00006-1.

[39] Merrick L., Taly A. The explanation game: explaining machine learning models using shapley values, 2020, p. 17–38. 10.1007/978-3-030-57321-8_2.

[40] Y. Nohara, K. Matsumoto, H. Soejima, N. Nakashima, Explanation of machine learning models using shapley additive explanation and application for real data in hospital, Comput. Methods Programs Biomed. 214 (2022) 106584, https://doi.org/10.1016/j.cmpb.2021.106584.

[41] D. Fryer, I. Strumke, H. Nguyen, Shapley values for feature selection: the good, the bad, and the axioms, IEEe Access. 9 (2021) 144352–144360, https://doi.org/10.1109/ACCESS.2021.3119110.

[42] M.R. Atelge, A.E. Atabani, J.R. Banu, D. Krisa, M. Kaya, C. Eskicioglu, et al., A critical review of pretreatment technologies to enhance anaerobic digestion and energy recovery, Fuel 270 (2020) 117494, https://doi.org/10.1016/J.FUEL.2020.117494.

[43] F. Passos, J. Carretero, I. Ferrer, Comparing pretreatment methods for improving microalgae anaerobic digestion: thermal, hydrothermal, microwave and ultrasound, Chem. Eng. J. 279 (2015) 667–672, https://doi.org/10.1016/J.CEJ.2015.05.065.

[44] I. TG, I. Haq, A.S. Kalamdhad, Factors affecting anaerobic digestion for biogas production: a review, Adv. Org. Waste Manag. Elsevier (2022) 223–233, https://doi.org/10.1016/B978-0-323-85792-5.00020-4.

[45] C. Mao, Y. Feng, X. Wang, G. Ren, Review on research achievements of biogas from anaerobic digestion, Renew. Sustain. Energy Rev. 45 (2015) 540–555, https://doi.org/10.1016/j.rser.2015.02.032.

[46] Y. Guo, Y. Zhao, Z. Li, Z. Wang, W. Zhang, K. Lin, et al., Exploring interactive effects of environmental and microbial factors on food waste anaerobic digestion performance: interpretable machine learning models, Bioresour. Technol. 416 (2025) 131762, https://doi.org/10.1016/J.BIORTECH.2024.131762.

[47] Y. Zhang, X. Yang, Y. Feng, Z. Dai, Z. Jing, Y. Li, et al., Accelerating integrated prediction, analysis and targeted optimization for anaerobic digestion of biomass after hydrothermal pretreatment using automated machine learning, Renew. Sustain. Energy Rev. 202 (2024) 114688, https://doi.org/10.1016/J.RSER.2024.114688.

[48] G. Kor-Bicakci, E. Ubay-Cokgor, C. Eskicioglu, Effect of dewatered sludge microwave pretreatment temperature and duration on net energy generation and biosolids quality from anaerobic digestion, Energy 168 (2019) 782–795, https://doi.org/10.1016/j.energy.2018.11.103.

[49] J.-C. Motte, R. Escudié, N. Bernet, J.-P. Delgenes, J.-P. Steyer, C. Dumas, Dynamic effect of total solid content, low substrate/inoculum ratio and particle size on solid-state anaerobic digestion, Bioresour. Technol. 144 (2013) 141–148, https://doi.org/10.1016/j.biortech.2013.06.057.

[50] Z.N. Abudi, Z. Hu, A.R. Abood, D. Liu, A. Gao, Effects of Alkali pre-treatment, total solid content, substrate to inoculum ratio, and pH on biogas production from Anaerobic digestion of mango leaves, Waste BioMass Valorization. 11 (2020) 887–897, https://doi.org/10.1007/s12649-018-0437-0.

[51] W.J. Park, J.H. Ahn, S. Hwang, C.K. Lee, Effect of output power, target temperature, and solid concentration on the solubilization of waste activated sludge using microwave irradiation, Bioresour. Technol. 101 (2010) S13–S16, https://doi.org/10.1016/J.BIORTECH.2009.02.062.

[52] A. Alhraishawi, S. Aslan, M. Ozturk, Methane production and struvite recovery from disintegrated biosludge at different microwave powers, Waste BioMass Valorization. (2025), https://doi.org/10.1007/s12649-025-02932-x.

[53] M.-Y. Yu, J.-P. Sun, S.-F. Li, J. Sun, X.-M. Liu, A.-Q. Wang, Effect of microwaves combined with peracetic acid to improve the dewatering performance of residual sludge, Environ. Sci. Pollut. Res. 31 (2024) 44885–44899, https://doi.org/10.1007/s11356-024-33931-5.

[54] L. Yue, J. Cheng, S. Tang, X. An, J. Hua, H. Dong, et al., Ultrasound and microwave pretreatments promote methane production potential and energy conversion during anaerobic digestion of lipid and food wastes, Energy 228 (2021) 120525, https://doi.org/10.1016/J.ENERGY.2021.120525.

[55] I. Arman, M. Athar, I.H. Farooqi, A. Kumar, Optimization of microwave intensified slaughterhouse sludge pretreatment method to enhance anaerobic digestion process by response surface methodology, BioMass Convers. Biorefin. (2024), https://doi.org/10.1007/s13399-024-05928-0.

[56] F. Long, L. Wang, W. Cai, K. Lesnik, H. Liu, Predicting the performance of anaerobic digestion using machine learning algorithms and genomic data, Water. Res. 199 (2021) 117182, https://doi.org/10.1016/J.WATRES.2021.117182.

[57] A. Gil, J.A. Siles, M.A. Martín, A.F. Chica, F.S. Estévez-Pastor, E. Toro-Baptista, Effect of microwave pretreatment on semi-continuous anaerobic digestion of sewage sludge, Renew. Energy 115 (2018) 917–925, https://doi.org/10.1016/j.renene.2017.07.112.

[58] Y.C. Bozkurt, O.G. Apul, Critical review for microwave pretreatment of waste-activated sludge prior to anaerobic digestion, Curr. Opin. Environ. Sci. Health 14 (2020) 1–9, https://doi.org/10.1016/j.coesh.2019.10.003.

[59] T.J. Appleton, R.I. Colder, S.W. Kingman, I.S. Lowndes, A.G. Read, Microwave technology for energy-efficient processing of waste, Appl. Energy 81 (2005) 85–113, https://doi.org/10.1016/j.apenergy.2004.07.002.

[60] R.J. Detz, B. van der Zwaan, Surfing the microwave oven learning curve, J. Clean. Prod. 271 (2020) 122278, https://doi.org/10.1016/j.jclepro.2020.122278.

[61] C. Leonelli, T.J. Mason, Microwave and ultrasonic processing: now a realistic option for industry, Chem. Eng. Process.: Process. Intensif. 49 (2010) 885–900, https://doi.org/10.1016/j.cep.2010.05.006.

[62] C. Tavera-Ruiz, J. Martí-Herrero, O. Mendieta, J. Jaimes-Estévez, P. Gauthier-Maradei, U. Azimov, et al., Current understanding and perspectives on anaerobic digestion in developing countries: colombia case study, Renew. Sustain. Energy Rev. 173 (2023) 113097, https://doi.org/10.1016/j.rser.2022.113097.

[63] L.C. Ampese, W.G. Sganzerla, D. Di, H. Ziero, A. Mudhoo, G. Martins, T. Forster-Carneiro, Research progress, trends, and updates on anaerobic digestion technology: a bibliometric analysis, J. Clean. Prod. 331 (2022) 130004, https://doi.org/10.1016/j.jclepro.2021.130004.

[64] P.M.V. Subbarao, T.C. D' Silva, K. Adlak, S. Kumar, R. Chandra, V.K Vijay, Anaerobic digestion as a sustainable technology for efficiently utilizing biomass in the context of carbon neutrality and circular economy, Environ. Res. 234 (2023) 116286, https://doi.org/10.1016/j.envres.2023.116286.

[65] C. Blanchard, P. Harris, C. Pocock, B.K. McCabe, Food and garden organic waste management in Australia: co-benefits for regional communities and local government, Sustainability 15 (2023) 9901, https://doi.org/10.3390/su15139901.

[66] H. Guo, J. Cui, J. Li, Biomass power generation in China: status, policies and recommendations, Energy Rep. 8 (2022) 687–696, https://doi.org/10.1016/j.egyr.2022.08.072.

[67] M. Banja, M. Jégard, V. Motola, R. Sikkema, Support for biogas in the EU electricity sector – A comparative analysis, BioMass BioEnergy 128 (2019) 105313, https://doi.org/10.1016/j.biombioe.2019.105313.

[68] K. Guerra, A. Welfle, R. Gutiérrez-Alvarez, M. Freer, L. Ma, P. Haro, The role of energy storage in Great Britain's future power system: focus on hydrogen and biomass, Appl. Energy 357 (2024) 122447, https://doi.org/10.1016/j.apenergy.2023.122447.

[69] S. Purswani, O. Norouzi, Overcoming challenges in the expanding RNG market: strategies and policies for stakeholders in the US, Energy Nexus. 13 (2024) 100270, https://doi.org/10.1016/j.nexus.2024.100270.

[70] O.C. Anika, S.G. Nnabuife, A. Bello, E.R. Okoroafor, B. Kuang, R. Villa, Prospects of low and zero-carbon renewable fuels in 1.5-degree net zero emission actualisation by 2050: a critical review, Carbon Capture Sci. Technol. 5 (2022) 100072, https://doi.org/10.1016/j.ccst.2022.100072.

[71] S. Bakkaloglu, J. Cooper, A. Hawkes, Life cycle environmental impact assessment of methane emissions from the biowaste management strategy of the United Kingdom: towards net zero emissions, J. Clean. Prod. 376 (2022) 134229, https://doi.org/10.1016/j.jclepro.2022.134229.

[72] M.O. Okwu, O.D. Samuel, O.B. Otanocha, P.P. Balogun, O.J. Tega, E. Ojo, Design and development of a bio-digester for production of biogas from dual waste, World J. Eng. 17 (2020) 247–260, https://doi.org/10.1108/WJE-07-2018-0249.